Published in final edited form as:
Cell Metab. 2009 May ; 9(5): 428–439. doi:10.1016/j.cmet.2009.04.001.

Ablation of ARNT/HIF1β in Liver Alters Gluconeogenesis, Lipogenic Gene Expression, and Serum Ketones

Xiaohui L. Wang[1], **Ryo Suzuki**[1], **Kevin Lee**[1], **Thien Tran**[1], **Jenny E. Gunton**[1,5], **Asish K. Saha**[2,3], **Mary-Elizabeth Patti**[1], **Allison Goldfine**[1], **Neil B. Ruderman**[2,3], **Frank J. Gonzalez**[4], and **C. Ronald Kahn**[1,*]

[1]Joslin Diabetes Center, Harvard Medical School, Boston, MA 02215, USA

[2]Diabetes Unit, Section of Endocrinology, Boston Medical Center, Boston, MA 02118, USA

[3]Departments of Medicine and Physiology, Boston University School of Medicine, Boston, MA 02118, USA

[4]Laboratory of Metabolism, National Cancer Institute, Bethesda, MD 20892, USA

[5]Diabetes and Transcription Factors, Garvan Institute of Medical Research, Sydney, Australia

SUMMARY

We have previously shown that expression of the transcription factor ARNT/HIF1β is reduced in islets of humans with type 2 diabetes. We have now found that ARNT is also reduced in livers of diabetics. To study the functional effect of its reduction, we created mice with liver-specific ablation (L-ARNT KO) using ARNT *loxP* mice and adenoviral-mediated delivery of Cre. L-ARNT KO mice had normal blood glucose but increased fed insulin levels. These mice also exhibited features of type 2 diabetes with increased hepatic gluconeogenesis, increased lipogenic gene expression, and low serum β-hydroxybutyrate. These effects appear to be secondary to increased expression of CCAAT/enhancer-binding protein alpha (C/EBPα), farnesoid X receptor (FXR), and sterol response element-binding protein 1c (SREBP-1c) and a reduction in phosphorylation of AMPK without changes in the expression of enzymes in ketogenesis, fatty acid oxidation, or FGF21. These results demonstrate that a deficiency of ARNT action in the liver, coupled with that in β cells, could contribute to the metabolic phenotype of human type 2 diabetes.

INTRODUCTION

The liver plays a major role in glucose and lipid homeostasis in both humans and rodents (Saltiel and Kahn, 2001; Michael et al., 2000). Hepatic glucose production is critical in the fasting state, providing fuel for the brain, renal medulla, and red blood cells. Initially, hepatic glucose is released from glycogen by the process of glycogenolysis, but after several hours of fasting, glucose production is primarily from gluconeogenesis, a process by which the liver produces glucose from precursors such as lactate and pyruvate (Pilkis and Granner, 1992;

*Correspondence: c.ronald.kahn@joslin.harvard.edu.

ACCESSION NUMBERS

The NCBI GEO accession number for the microarray data reported in this paper is GSE15653.

SUPPLEMENTAL DATA

Supplemental Data include Supplemental Experimental Procedures, one table, and four figures and can be found online at http://www.cell.com/cell-metabolism/supplemental/S1550-4131(09)00092-8.

The authors declare that they have no competing financial interests.

Cherrington et al., 1998). In addition, fatty acid β-oxidation is activated during fasting, providing ATP for the liver (Postic et al., 2004) and generating ketone bodies, which provide an alternative fuel source for the brain and heart (Blazquez et al., 1999). Gluconeogenesis, fatty acid β-oxidation, and ketogenesis are all suppressed by insulin. In pathological states, such as type 1 diabetes mellitus, elevated gluconeogenesis and ketogenesis contribute significantly to hyperglycemia and hyperketonemia. One unexplained and interesting finding is that in type 2 diabetes, where insulin resistance predominates, gluconeogenesis is increased without an obvious increase in ketogenesis (Cherrington et al., 1998).

Multiple transcription factors and coregulators have been identified as the downstream targets of insulin signaling in the regulation of gluconeogenesis, lipogenesis, and fatty acid oxidation in the liver, including the peroxisome proliferator-activated receptors (PPARs), the PPAR coactivators PGC-1α and PGC-1β, forkhead box O1 (FoxO1), farnesoid X receptor (FXR), sterol response element-binding protein 1c (SREBP-1c), and CCAAT/enhancer-binding proteins (C/EBPs) (Pedersen et al., 2007; Qiao et al., 2006; Sinal et al., 2000; Foufelle and Ferre, 2002; Horton et al., 2002; Puigserver et al., 2003; Yoon et al., 2001). These proteins function either cooperatively or in parallel in the regulation of expression of genes in glucose and lipid metabolism. To date, the upstream regulators of the key transcription factors involved in control of glucose, lipid, and ketone homeostasis in the diabetic state remain largely unknown.

The aryl hydrocarbon receptor nuclear translocator (ARNT), also known as hypoxia-inducible factor 1β (HIF1β), is a ubiquitously expressed nuclear protein that belongs to the basic helix-loop-helix (bHLH)/PAS family of transcription factors (Reisz-Porszasz et al., 1994). ARNT is a heterodimerization partner for several members of the bHLH transcription factor family. The most extensively studied include the aryl hydrocarbon receptor (AHR), which responds to exogenous organic molecules, such as dioxins; and HIF1α, which is regulated by cellular oxygen tension (Semenza, 1999; Ema et al., 1997). With its cognate heterodimer partners, ARNT regulates a wide range of processes involving detoxification of organic molecules, response to hypoxia, development of the vascular system, cell proliferation, and control of glycolytic enzymes (Semenza, 1999; Ema et al., 1997).

Previous studies from our laboratory have demonstrated reduced expression of ARNT in β cells in humans with type 2 diabetes and provided evidence that this reduction contributes to impaired insulin secretion in type 2 diabetes (Gunton et al., 2005). In the present study, we found that ARNT expression was also reduced in liver of obese individuals with type 2 diabetes. We further demonstrated that liver-specific knockout of the ARNT/HIF1β increases the expression of key lipogenic and gluconeogenic enzymes, resulting in increased gluconeogenesis and dyslipidemia but low levels of circulatory ketones. Such effects appear to be mediated by activation of key transcription factors in gluconeogenesis and lipogenesis, including SREBP-1c, FXR, and C/EBPα. Together, these results suggest that ARNT plays important roles in the control of metabolism in β cells and liver, and that alterations in ARNT expression in liver may lead to dysregulation of glucose homeostasis and lipid metabolism without increased ketogenesis.

RESULTS

Reduced Expression of ARNT in the Livers of Humans with Type 2 Diabetes and Mice with STZ-Induced Diabetes

Microarray analysis was performed to assess expression of ARNT in liver specimens from normal lean individuals, obese individuals, and obese type 2 diabetics. Expression of ARNT mRNA was not altered in obese subjects without diabetes mellitus (DM), but was reduced in obese type 2 diabetic patients with both well-controlled (DM [W]) and poorly-controlled (DM

[P]) blood glucose levels (Figure 1A). Although these differences did not reach statistical significance in each diabetic group due to the small sample size, when considered together, the data demonstrated an average 30% decrease in the expression of ARNT mRNA in the liver of obese individuals with type 2 diabetes ($p < 0.02$). As shown in Table 1, blood glucose concentrations and fasting insulin levels were higher in the DM (W) and DM (P) groups compared to the lean controls ($p < 0.05$). Thus, high glucose levels, high insulin levels, and insulin resistance are associated with the reduced expression of ARNT in the livers of humans with type 2 diabetes.

To determine the effects of insulin and glucose in the regulation of ARNT, streptozocin (STZ)-induced diabetic mice were studied. The glucose levels in these mice were elevated 4-fold over control (564 ± 9.8 versus 139 ± 7.8 mg/dl, $p < 0.005$), while insulin levels were almost undetectable. Expression of ARNT protein in STZ diabetic mice was reduced to 63% ± 9% of Control levels ($p < 0.004$), and this was largely restored to baseline upon insulin treatment (Figure 1B), suggesting that insulin signaling activates the expression of the ARNT gene and that ARNT expression is reduced in both insulin-deficient and insulin-resistant states.

Insulin, but Not Glucose, Increases the Expression and Nuclear Translocation of ARNT

To determine whether the regulation of ARNT expression is a direct effect of glucose or insulin, human hepatoblastoma Huh7 cells were exposed for 16 hr to either low (5 mM) or high (25 mM) glucose and 0, 10, or 100 nM insulin and analyzed for ARNT expression by western blotting. No changes in the expression of ARNT were observed at the different glucose concentrations (Figure 1C); however, pretreatment for 16 hr with insulin at 10 and 100 nM increased the expression of ARNT protein to 120% and 130% of Control, respectively (Figure 1D, $p < 0.05$).

To further determine whether subcellular distribution of ARNT protein is regulated by glucose or insulin, Huh7 cells were exposed for 5 min to D-glucose (dextrose) at different concentrations, 22 mM L-glucose, or 100 nM insulin. Neither D- nor L-glucose changed nuclear translocation of ARNT protein (Figure 1E). However, when Huh7 cells were treated with insulin for 5 min and then subjected to fraction, there was a clear translocation of ARNT protein from the cytoplasm to the nuclear fraction (Figure 1E). Insulin-induced ARNT nuclear translocation was also observed by immunofluorescent staining. Thus, in the basal state, ARNT protein was mainly located in the cytoplasm of Huh7 cells (Figure 1F, subpanels a and c). When these cells were treated with insulin at 10 and 100 nM (Figure 1F, subpanels c and d) individually for 5 min, ARNT protein translocated into the nucleus. Thus, insulin can increase the expression and the nuclear translocation of ARNT protein in liver. By contrast, glucose does not directly regulate the expression or nuclear translocation of ARNT.

Acute Ablation of ARNT in Mouse Liver (L-ARNT KO)

To define the potential effects of reduced ARNT expression in the liver, we created an acute postnatal liver-specific ablation of ARNT by tail-vein injection of an adenovirus carrying Cre recombinase (Ad-Cre) into mice carrying two copies of the ARNT gene in which exon 6 was flanked by *loxP* sites (flox/flox mice) to create the L-ARNT KO mouse (Tomita et al., 2000). Same age and sex ARNT flox/flox mice were injected with Ad-CMV vector as controls (Control). Three independent groups of five or six pairs of mice (age 9–11 months) were studied between days 4 and 6 after the adenoviral injection to determine the effect of acute ARNT deletion on metabolism and gene and protein expression. One was a group of six pairs of female mice on normal chow diet (FNC). The second group consisted of five pairs of male mice on normal chow diet (MNC). The third group represents six pairs of female mice on high-fat (60%) diet for 3 months (FHF).

To determine the efficacy of Ad-Cre recombination of the ARNT gene, real-time RT-PCR was performed to quantify ARNT mRNA in liver of all three groups of mice 6 days after adenovirus injection, using TBP mRNA as the normalization control. Expression of ARNT mRNA was reduced to 37% ± 5% of control levels in the liver of the FNC group (Figure 2A) and to 26% ± 3% and 24% ± 4% of Control in the liver of the MNC and FHF mice ($p < 0.00005$). Consistent with the mRNA results, expression of ARNT protein was undetectable by western blot of livers of L-ARNT KO mice from the FNC group (Figure 2B), as well as in the livers of MNC and FHF mice.

L-ARNT KO Induces Insulin Secretion and Hepatic Gluconeogenesis

When compared to levels prior to initiation of the experiment, there were slight reductions in body weight and food intake in both L-ARNT KO and Control mice after adenovirus injection. However, there were no significant differences in body weight or food intake between L-ARNT KO and Control mice in any of the three groups (Figure S1A) on day 6 after the adenovirus injection; there was no difference in blood glucose levels between L-ARNT KO mice and Control in either of the FNC or MNC groups on normal chow (Figure 2C). However, a small but statistically significant increase in fed blood glucose levels was observed in L-ARNT KO mice from the FHF group compared with Control (127.6 ± 5.0 mg/dl versus 106.4 ± 7.6 mg/dl; $p < 0.05$) (Figure 2C). Fed insulin levels of Control and L-ARNT KO mice were 0.25 ± 0.05 ng/dl versus 0.48 ± 0.14 ng/dl in the FNC group and 1.51 ± 0.77 ng/dl versus 3.30 ± 1.14 ng/dl in the MNC group and were significantly increased from 0.62 ± 0.11 ng/dl to 1.20 ± 0.20 ng/dl in the FHF group ($p = 0.04$) (Figure 2D). Increased fed insulin levels with normal to higher blood glucose levels in the L-ARNT KO mice were observed in each of the three independent experimental groups.

To better assess the effect of L-ARNT KO on the whole-body glucose utilization, intraperitoneal glucose tolerance tests (GTTs) were performed in the FNC, FHF, and MNC groups (Figure 2E). Integrated glucose concentrations were calculated as the area under the curve (AUC). Overall, no significant differences in the AUC were observed in either the FNC or FHF groups (Figure S1B). Thus, the higher serum insulin levels were able to compensate for the insulin resistance in female L-ARNT KO mice. GTT tests in L-ARNT KO mice from the MNC group, on the other hand, revealed a significant increase in glucose values at all points from 15 to 120 min (Figure 2E).

To directly examine the effect of deficiency of ARNT on hepatic glucose output, pyruvate challenge experiments were performed using the FHF and MNC groups. By measuring blood glucose in response to the administration of pyruvate, a major gluconeogenic substrate, one gets an estimation of gluconeogenic potential in vivo. Following pyruvate administration in Control mice from the FHF group, blood glucose concentrations increased by 46 mg/dl over basal levels at 15 min ($p < 0.005$), plateaued, and then decreased after 60 min. Glucose concentrations in LARNT KO mice were higher at all time points: 138 ± 9.5 mg/dl versus 107 ± 4.5 mg/dl at 15 min ($p = 0.02$), 120.7 ± 6.2 mg/dl versus 85.6 ± 8.1 mg/dl at 30 min ($p = 0.01$), and 66.2 ± 7.2 mg/dl versus 48 ± 6.7 mg/dl at 60 min ($p = 0.10$) (Figure 2F). The area under the serum glucose curve following the pyruvate challenge in the FHF group of L-ARNT KO mice was increased 34% compared to the Control ($p < 0.02$) (Figure 2G). In the MNC group, glucose concentrations in L-ARNT KO versus Control mice were also higher by 40%–50% at the 15, 50, and 60 min time points ($p = 0.06$, 0.01, and 0.05, respectively) (Figure 2F). The AUC in the MNC group of L-ARNT KO mice was also increased by 41% ($p < 0.05$) (Figure 2G). Taken together, these results indicate L-ARNT KO mice have significantly increased ability to convert pyruvate to glucose, i.e., higher hepatic gluconeogenesis, than normal mice.

Insulin Sensitivity and Hepatic Glucose Production by Hyperinsulinemic-Euglycemic Clamp

To measure more precisely whole-body insulin sensitivity and hepatic glucose production, we performed hyperinsulinemic-euglycemic clamps with D-[3-^{3}H]glucose in the FNC group. At the time of this procedure, there was no significant difference in body weight (40.3 ± 2.1 g versus 38.7 ± 1.9 g) or fasting glucose levels (104 ± 5 mg/dl versus 106 ± 1 mg/dl) between the Control and L-ARNT KO mice. Whole-body insulin sensitivity, as quantified by the glucose infusion rate during the hyperinsulinemic-euglycemic clamp, was reduced in the L-ARNT KO mice (n = 5) to 22.9 ± 2.8 mg/kg/min, compared with 27.2 ± 4.5 mg/kg/min in the Controls (n = 6), suggesting mild whole-body insulin resistance (Figure 2H). Interestingly, basal hepatic glucose production was also increased in the L-ARNT KO mice, from 53 ± 12 mg/kg/min to 72 ± 21 mg/kg/min (Figure 2I). Although this difference did not quite reach statistical significance, when considered along with the increased response to the pyruvate challenge, this finding is consistent with increased basal gluconeogenesis in the L-ARNT KO mice. During the hyperinsulinemic-euglycemic clamp, insulin suppressed hepatic glucose production in both the L-ARNT and Control groups to a similar extent (82% ± 6.2% versus 71% ± 7.3%) (Figure 2I).

Potential Mechanisms of Increased Hepatic Gluconeogenesis in L-ARNT KO Mice

To determine the mechanisms of increased hepatic gluconeogenesis caused by L-ARNT KO, the mRNA expression levels of key gluconeogenic enzymes, including phosphoenolpyruvate carboxykinase (PEPCK), fructose 1,6-bisphosphatase (FBP1), and glucose 6-phosphatase (G6Pase), were measured in fed Control and L-ARNT KO mice. As shown in Figure 3A, expression levels of PEPCK and G6Pase mRNAs were increased 3- to 5-fold and 1.5- to 3-fold in the livers of L-ARNT KO mice compared with fed Control in each of the three experimental groups (Figure 3A). The expression level of FBP1 mRNA was also significantly increased in the livers of L-ARNT KO mice from both the FNC and MNC groups, but not from the FHF group. Thus, the increased hepatic gluconeogenesis in L-ARNT KO mice was the result of increased expression of key gluconeogenic enzymes.

It is known that many transcription factors and coactivators, including hepatocyte nuclear factor α (HNF-4α), FoxA2/HNF-3β, FoxO1, PGC-1α, CREB, and C/EBPα, are involved in the regulation of the PEPCK gene (Roesler et al., 1989; Pilkis and Granner, 1992; Yoon et al., 2001). Many of these transcription factors and coregulators are also involved in the regulation of other key gluconeogenic enzymes, such as G6Pase (Schmoll et al., 1999; Onuma et al., 2006). To determine whether ARNT regulates the expression of the gluconeogenic enzymes through the regulation of these key transcription factors, expression of genes encoding these factors was studied in the liver samples of L-ARNT KO and control mice under fed conditions. No significant differences were found in the expression of mRNA levels of CREB, FoxA2, FoxO1, HNF-4α, PGC-1α, and PGC-1β genes in the livers of the L-ARNT KO mice from the FNC group (Figures 3B). Interestingly, there was a two-fold induction of C/EBPα mRNA, but not the expression of C/EBPβ and C/EBPδ, in the livers of L-ARNT KO mice, and this was paralleled by a 2-fold increase in C/EBPα protein (Figure 3C). Similar results were observed in the MNC group (Figure S2). The possibility that the L-ARNT KO activates gluconeogenesis through activation of the expression of C/EBPα gene is consistent with the growing body of literature showing that C/EBPα is involved in the regulation of gluconeogenesis and lipid metabolism in the liver (Pedersen et al., 2007; Qiao et al., 2006).

L-ARNT KO Increases Hepatic Lipogenesis but Reduces Hepatic Lipid Storage

To determine the effect of L-ARNT KO on lipid metabolism, concentrations of cholesterol, triglyceride (TG), and free fatty acids (FFA) were measured in the serum of L-ARNT KO mice from each experimental group 6 days after the adenovirus injection (Figure 4A). No significant changes were observed in fed cholesterol levels in L-ARNT KO mice from each group

compared with Control (Figure 4A). Fed TG concentrations in the serum of L-ARNT KO mice from the FHF group were significantly reduced compared with Control ($p < 0.01$). Fed serum FFA levels of L-ARNT KO mice versus Control from the FNC group were also significantly reduced ($p < 0.004$). A trend for a similar reduction of fed FFA concentration was seen in L-ARNT KO mice from the FHF group. Fasting FFA concentrations in L-ARNT KO mice from the MNC group were also significantly reduced compared with Control ($p < 0.05$) (Figure 4B).

We further determined the effect of L-ARNT KO on hepatic lipid metabolism by assessing hepatic lipid content and lipid distribution. Total liver TG content was reduced by 50% in the MNC group but not in the FNC group (Figure 4C). When de vivo hepatic fatty acid and TG synthesis were measured using tritiated water, there were no significant differences between L-ARNT KO mice and Control (Figure 4D). Interestingly, however, on oil red O staining (Figure 4E), the lipid droplets in the livers of L-ARNT KO mice from both the FNC and MNC groups were noticeably smaller when compared with the lipid droplets in the Control. Thus, ARNT deletion converts fat storage from a macrovesicular pattern to a microvesicular pattern. It is known that the PAT family proteins (perilipin, adipose differentiation-related protein [ADRP], and tail-interacting protein of 47 kDa [TIP47]) contribute to formation and function of lipid storage droplets (Londos et al., 2005). ADRP and TIP47 were expressed abundantly in liver. Gene expression analysis revealed a trend toward reduction of ADRP gene in the livers of both male and female L-ARNT KO mice compared to Control, but neither of these changes reached statistical significance (Figure S3).

Alterations in Genes Controlling Hepatic Lipogenesis in the L-ARNT KO Mice

Changes in serum lipid levels and hepatic lipids were secondary to changes in genes and transcriptional regulators of hepatic lipogenesis. Thus, the expression of SCD1 and FAS mRNAs in the livers of fed L-ARNT KO mice were increased 2- to 7-fold compared with Control in each of the three groups (Figure 4F). Similarly, the expression of FAS protein in the livers of L-ARNT KO mice from the MNC group was also increased 1.5-fold (Figure 4G). On the other hand, there were no significant differences in the expression of the genes encoding transcription factors involved in the regulation of hepatic lipogenesis, including LXR, PPARα, PPARγ, and SREBP-1α, in the livers of L-ARNT KO mice of either the FNC (Figure 4H) or MNC group (data not shown). However, there was a 2-fold induction in the expression of SREBP-1c and FXR genes in the livers of L-ARNT KO mice from both of these groups (Figure 4H and Figure S2), as well as the 2-fold increase in C/EBPα shown above. The SREBP-1c protein is synthesized in endoplasmic reticulum and further processed in the Golgi apparatus, where proteases liberate the N-terminal mature forms that translocate to the nucleus to activate lipogenic genes. The level of mature forms of SREBP-1c protein was significantly increased in the hepatic nuclear extract of L-ARNT KO mice from the MNC group (Figure 4I). Thus, three transcription factors (FXR, SREBP-1c, and C/EBPα) involved in the regulation of hepatic lipogenesis (Pedersen et al., 2007; Qiao et al., 2006; Sinal et al., 2000; Foufelle and Ferre, 2002; Horton et al., 2002; Puigserver et al., 2003) are increased in the L-ARNT KO mice and could contribute to the increased hepatic lipogenesis.

L-ARNT KO Reduces Serum β-Hydroxybutyrate Levels

Ketone bodies, including β-hydroxybutyrate (β-OHB), are mainly generated in liver from serum FFA as a result of β-oxidation and ketogenesis (Blazquez et al., 1999). Despite similar food intake, L-ARNT KO mice exhibit significantly decreased fed serum β-OHB levels. In the FNC group, fed β-OHB levels from L-ARNT KO mice versus Control were 0.64 ± 0.05 mM versus 0.37 ± 0.07 mM ($p = 0.01$). In the FHF and MNC groups, fed serum β-OHB levels from L-ARNT KO mice were lower than in Controls; however, they did not reach significance due to the large variation (Figure 5A). Under fasting conditions, however, serum β-OHB levels from the MNC group of L-ARNT KO mice were significantly lower than Control (Figure 5B).

Interestingly, these changes in serum ketone levels in the L-ARNT KO mice occurred with no significant alteration in expression of genes encoding key enzymes in fatty acid β-oxidation or hepatic ketogenesis (Figure S4 and Table S1).

AMP-activated protein kinase (AMPK) plays a regulatory role in the control of fatty acid β-oxidation. Phosphorylation of AMPK activates fatty acid β-oxidation through phosphorylation of ACC1 (Blazquez et al., 1999; Ruderman et al., 2003; Musi, 2006; Assifi et al., 2005). Western blot analysis revealed no differences in expression of AMPK protein in the livers of L-ARNT KO mice compared with fed Control in both the FNC and MNC groups (Figure 5C). Interestingly, there was a 40% reduction of phosphorylated AMPK (p-AMPK) in livers of male L-ARNT KO mice and a 20% reduction of p-AMPK from the FNC group (Figures 5C and 5D). However, this was not accompanied by a change in phosphorylation status of ACC1, a marker of AMPK activity (Figure 5C).

Malonyl-CoA inhibits fatty acid β-oxidation by inhibition of Carnitine Palmitoyltransferase I (CPT-I) activity (McGarry et al., 1983; Ruderman et al., 2003). To determine whether L-ARNT KO affects hepatic malonyl-CoA production, liver extracts from both L-ARNT KO mice and Control mice were measured radioenzymatically. Malonyl-CoA levels were slightly increased in the livers of L-ARNT KO mice from both the FNC and MNC groups compared with Control; however, these did not reach statistical significance (Figure 4E). While modest, the reduced p-AMPK and slightly increased malonyl-CoA levels may account for the reduction of serum β-OHB levels.

Recently, studies from two laboratories have shown that growth factor FGF21 is involved in control of ketone body formation and that FGF21 transgenic mice exhibit increased ketogenesis (Inagaki et al., 2007; Badman et al., 2007). While FGF21 mRNA levels were detected in liver of L-ARNT mice, there was no significant change in the expression of FGF21 gene in these livers compared with Control (Figure 5F).

DISCUSSION

In this study, we have shown that there is a reduction in expression of ARNT in livers of humans with type 2 diabetes. When the effect of this reduction of ARNT was assessed by acute ablation of the ARNT gene in the liver of mice, we found an increase in gluconeogenesis and lipogenesis, an increase in serum insulin levels, and a relative decrease in ketogenesis. These findings in L-ARNT KO mice mimic those of human type 2 diabetes, suggesting that a deficiency of ARNT action in the liver could contribute to the altered metabolic function in humans with type 2 diabetes. In previous studies, we have shown that individuals with type 2 diabetes have a marked reduction of ARNT expression in pancreatic islets, which when modeled in cells and mice leads to impaired glucose-stimulated insulin secretion and glucose intolerance (Gunton et al., 2005). Taken together, these results suggest that reductions in ARNT expression in the β cell and liver may play important roles in the defects observed in human type 2 diabetes in glucose homeostasis and lipid metabolism.

The effects of reduction in ARNT on hepatic gluconeogenesis and lipogenesis are mediated by elevated expression of key gluconeogenic and lipogenic enzymes, including PEPCK, G6Pase, SCD1, and FAS. Studies from multiple research groups have shown that the rate-limiting enzymes involved in gluconeogenesis and lipogenesis are mainly regulated at the transcriptional level by a number of transcription factors and their coregulators (Pedersen et al., 2007; Qiao et al., 2006; Sinal et al., 2000; Foufelle and Ferre, 2002; Horton et al., 2002; Puigserver et al., 2003; Yoon et al., 2001). C/EBPα is essential for the activation of hepatic glucose production at birth, and disruption of the C/EBPα gene in mice causes hypoglycemia associated with the impaired expression of the gluconeogenic enzymes PEPCK and G6Pase

(Pedersen et al., 2007; Qiao et al., 2006). Acute knockout of C/EBPα also significantly reduces the expression of lipogenic genes, including ACC, SCD1, and FAS (Pedersen et al., 2007; Qiao et al., 2006). These effects occur through C/EBPα binding to its binding element on these gene promoters (Pedersen et al., 2007; Schmoll et al., 1999). ARNT appears to function as an upstream regulator of C/EBPα, such that knockout of ARNT increases C/EBPα gene expression, which in turn activates the expression of gluconeogenic and lipogenic enzymes.

Besides the increase in C/EBPα gene expression, acute knockout of ARNT also increases the expression of FXR and SREBP-1c, two important regulators of lipid homeostasis (Sinal et al., 2000; Foufelle and Ferre, 2002; Horton et al., 2002). SREBP-1c mRNA is the predominant isoform in liver and is a member of the bHLH family of DNA binding proteins that form dimers that recognize the inverted E-box repeats. SREBP-1c mRNA expression is controlled in part by insulin, increased by a fasting and refeeding regimen, and decreased in rats with STZ-induced diabetes. Overexpression of SREBP-1c in liver prevented the downregulation of lipogenic genes during fasting via upregulation of the genes controlling fatty acid synthesis (Jump et al., 2005). Thus, acute knockout of ARNT activates the expression of C/EBPα and SREBP-1c genes. Identifying ARNT as an upstream regulator of SREBP-1c and C/EBPα genes may cast some light on the regulation of glucose and lipid homeostasis in the liver.

Insulin signaling plays an important role in the regulation of hepatic glucose homeostasis (Saltiel and Kahn, 2001; Michael et al., 2000). Mice with liver-specific insulin receptor knockout (LIRKO) exhibit dramatic insulin resistance, severe glucose intolerance, and a failure of insulin to suppress hepatic glucose production due to increased PEPCK and G6Pase gene expression (Michael et al., 2000). Interestingly, L-ARNT KO mice exhibit a similar but milder phenotype compared to LIRKO mice with unsuppressed hepatic gluconeogenesis and hyperinsulinemia. LIRKO mice, however, exhibit reduced expression of SREBP-1c and FXR (Biddinger et al., 2008), which clearly distinguishes them from the L-ARNT KO mice and points to different forms of hepatic insulin resistance created by these two pathways.

L-ARNT KO mice also exhibit hypoketonemia, a feature not observed in LIRKO mice. It is believed that anabolic effects of the relatively high insulin concentrations in type 2 diabetes cause reduced fatty acid β-oxidation in the liver, which prevents the formation of ketone bodies. The hypoketonemia in L-ARNT mice could, therefore, be due in part to the hyperinsulinemia of these mice. AMP-activated protein kinase (AMPK) is the primary regulator of the cellular response to reduced ATP levels and may also play a role in the reduced ketogenesis (Ruderman et al., 2003; Musi, 2006; Assifi et al., 2005). AMPK is an important metabolic switch, phosphorylating key target proteins that lead to stimulation of hepatic fatty acid oxidation and ketogenesis, inhibition of cholesterol synthesis, lipogenesis, and TG synthesis (Ruderman et al., 2003; Musi, 2006; Assifi et al., 2005). Phosphorylation of AMPK was reduced in L-ARNT KO mice, which could contribute to reduced fatty acid oxidation and reduced formation of ketone bodies while allowing increased function of the enzymes in the lipogenic pathway. Recent studies have shown that FGF21 is involved in control of ketone body formation (Inagaki et al., 2007; Badman et al., 2007). Mice on a ketogenic diet have increased FGF21 expression, and FGF21 transgenic mice exhibit increased ketogenesis. However, there was no change in the expression of FGF21 gene in L-ARNT KO mice compared to control. Thus it appears likely that the reduced formation of β-OHB in L-ARNT KO mice is the product of the anabolic effects of hyperinsulinemia and the reduction of phosphorylation of AMPK.

One of the most interesting findings in the L-ARNT KO mice was the reduced size of the lipid droplets in their livers. It is known that lack of PAT family proteins reduces the size of lipid droplets (Londos et al., 2005). L-ARNT mice have a trend to reduced levels of ADRP, one of the PAT proteins, in their livers, which may contribute to the reduced size of the lipid droplets, although this effect is very modest.

The exact molecular mechanism of ARNT action on hepatic metabolism may be complex. ARNT is a member of the bHLH/PAS family of proteins (Reisz-Porszasz et al., 1994). ARNT functions through heterodimerization with AHR in the toxic effect of dioxin. Within the nucleus, AHR/ARNT heterodimers bind to specific DNA response elements with the consensus motif TNGTGTG of the target promoter to control gene transcription. The other dimerization partners of ARNT include SIM1 and SIM2 (regulators of neurogenesis) and HIF1α and HIF2α (regulators of the cellular response to hypoxia) (Semenza, 1999; Ema et al., 1997). Thus, ARNT may play a role in regulating many different signaling pathways by partnering with different transcription factors. Studies on overexpression of ARNT partners are needed to gain more insight into the mechanisms of ARNT action in the liver.

The metabolic syndrome shares a number of features of type 2 diabetes and is also increasing at an alarming rate, with almost 25% of the adult U.S. population currently affected. Given the fact that the metabolic syndrome and type 2 diabetes increase the risk of many other conditions, including nonalcoholic fatty liver and cardiovascular disease, more specific and effective therapeutic strategies are urgently needed. Certain ligand-activated nuclear receptors, including FXR, SREBP-1c, and C/EBPα, provide promising new targets for this purpose. Since ARNT/HIF1β acts as an upstream regulator of FXR, SREBP-1c, and C/EBPα genes in the regulation of insulin-mediated inhibition on gluconeogenesis and lipogenesis (Figure 6), approaches to modulate ARNT levels or its transcriptional effects could provide a novel approach for treatment of diabetes, fatty liver, and the metabolic syndrome.

EXPERIMENTAL PROCEDURES

Animals, Adenoviruses, and Plasma/Serum Biochemical Measurements

ARNT flox/flox mice were generated as previously described (Tomita et al., 2000). Three groups of ARNT flox/flox mice were studied: male and female mice (9–11 months) on normal chow diet (MNC and FNC, respectively) and female mice (9 months) that had been on a 60% high-fat diet for 3 months (FHF). In each group, half of the mice were injected with the adenoviral-Cre construct and half with a control adenovirus via the tail vein 4–6 days prior to the experiments.

Glucose Tolerance and Pyruvate Challenge Tests

For GTT, ARNT flox/flox and L-ARNT KO mice deprived of food for 16 hr were injected intraperitoneally (i.p.) with glucose (2 g/kg body weight), and glucose from tail vein blood was measured at 0–120 min using a glucometer. For the pyruvate challenge test, 16 hr fasted mice were injected i.p. with pyruvate (2 g/kg) dissolved in saline, and glucose was measured as above.

Hyperinsulinemic-Euglycemic Clamp Experiments

The jugular vein of ARNT flox/flox mice was cannulated. After a 2 day recovery period, Cre and control adenovirus were injected. After an additional 5 days and a 4 hr fast, a hyperinsulinemic-euglycemic clamp was performed with D-[3-^{3}H]glucose as described by Norris et al., 2003, using a continuous insulin infusion of 3.5 mU/kg/min. The adenoviral injection and the clamp technique were carried out without knowledge, i.e., blinded of the genotype until all calculations were completed. Hepatic glucose production was assessed by subtraction of the glucose infusion rate from whole-body glucose turnover as measured with D-[3-^{3}H]glucose.

Hepatic De Novo Lipogenesis

ARNT flox/flox and L-ARNT KO mice were injected with 0.5 mCi of ^3H_2O (0.4ml of 1.25 mCi/ml). The rate of hepatic de novo lipogenesis was determined by measuring the amount of newly synthesized FA and TG present in the liver 1 hr after the i.p. injection. ^{3}H-labeled fatty acids were isolated by saponification of liver samples in KOH. After extraction of nonsaponifiable lipids and acidification with H_2SO_4, the ^{3}H-labeled fatty acids were extracted with chloroform and separated by thin layer chromatography. The plate was stained with primulin. The FA and TG spots were scraped off the plate, added to scintillation fluid, and counted in a liquid scintillation counter. The specific activity of body water was determined and used to calculate de novo lipogenesis as micromoles of ^3H_2O incorporated into FA/hr/g and TG/hr/g of liver tissue.

Quantification of Hepatic Malonyl-CoA and TG Contents

Liver tissues were removed from ARNT flox/flox and L-ARNT KO mice and immediately frozen in liquid nitrogen. Liver was homogenized and deproteinized with 10% perchloric acid, the filtrate was neutralized (Saha et al., 1997), and malonyl CoA was determined radioenzymatically by a modification of the method of McGarry (McGarry et al., 1978). For the measurement of hepatic TG content, 0.1–0.2 g of liver tissue from each mouse was homogenized in 500 μl buffer containing 150 mM NaCl and 10 mM Tris (pH 7.5) and extracted with 400 μl methanol and 800 μl chloroform. The chloroform layer, containing TG, was evaporated overnight and resuspended in 70% ethanol; TG was measured enzymatically and expressed relative to protein content.

Statistics

The results are expressed as means ± SEM. Significance was established using the Student's t test and analysis of variance when appropriate. Differences were considered significant at $p < 0.05$. Two-way ANOVA with repeat measurements was performed to analyze measurements obtained by time course.

Supplementary Material

Refer to Web version on PubMed Central for supplementary material.

Acknowledgments

This work was supported by the Diabetes Genome Anatomy Project Grants DK-060837, DK-067509, and PO1HL68758 and the Mary K. Iacocca Professorship. We acknowledge Doctor Londos for providing advice regarding lipid droplets, Doctor Daryl K. Granner for his suggestions on hepatic gluconeogenesis, and members of the Kahn and Kulkarni labs for their helpful discussions.

REFERENCES

Assifi MM, Suchankova G, Constant S, Prentki M, Saha AK, Ruderman NB. AMP-activated protein kinase and coordination of hepatic fatty acid metabolism of starved/carbohydrate-refed rats. Am. J. Physiol. Endocrinol. Metab 2005;289:E794–E800. [PubMed: 15956049]

Badman MK, Pissios P, Kennedy AR, Koukos G, Flier JS, Maratos-Flier E. Hepatic fibroblast growth factor 21 is regulated by PPARalpha and is a key mediator of hepatic lipid metabolism in ketotic states. Cell Metab 2007;5:426–437. [PubMed: 17550778]

Biddinger SB, Hernandez-Ono A, Rask-Madsen C, Haas JT, Alemán JO, Suzuki R, Scapa EF, Agarwal C, Carey MC, Stephanopoulos G, et al. Hepatic insulin resistance is sufficient to produce dyslipidemia and susceptibility to atherosclerosis. Cell Metab 2008;7:125–134. [PubMed: 18249172]

Blazquez C, Woods A, de Ceballos ML, Carling D, Guzman M. The AMP-activated protein kinase is involved in the regulation of ketone body production by astrocytes. J. Neurochem 1999;73:1674–1682. [PubMed: 10501215]

Cherrington AD, Edgerton D, Sindelar DK. The direct and indirect effects of insulin on hepatic glucose production in vivo. Diabetologia 1998;41:987–996. [PubMed: 9754815]

Ema M, Taya S, Yokotani N, Sogawa K, Matsuda Y, Fujii-Kuriyama Y. A novel bHLH-PAS factor with close sequence similarity to hypoxiainducible factor 1alpha regulates the VEGF expression and is potentially involved in lung and vascular development. Proc. Natl. Acad. Sci. USA 1997;94:4273–4278. [PubMed: 9113979]

Foufelle F, Ferre P. New perspectives in the regulation of hepatic glycolytic and lipogenic genes by insulin and glucose: a role for the transcription factor sterol regulatory element binding protein-1c. Biochem. J 2002;366:377–391. [PubMed: 12061893]

Gunton JE, Kulkarni RN, Yim S, Okada T, Hawthorne WJ, Tseng YH, Roberson RS, Ricordi C, O'Connell PJ, Gonzalez FJ, Kahn CR. Loss of ARNT/HIF1beta mediates altered gene expression and pancreatic-islet dysfunction in human type 2 diabetes. Cell 2005;122:337–349. [PubMed: 16096055]

Horton JD, Goldstein JL, Brown MS. SREBPs: activators of the complete program of cholesterol and fatty acid synthesis in the liver. J. Clin. Invest 2002;109:1125–1131. [PubMed: 11994399]

Inagaki T, Dutchak P, Zhao G, Ding X, Gautron L, Parameswara V, Li Y, Goetz R, Mohammadi M, Esser V, et al. Endocrine regulation of the fasting response by PPARalpha-mediated induction of fibroblast growth factor 21. Cell Metab 2007;5:415–425. [PubMed: 17550777]

Jump DB, Botolin D, Wang Y, Xu J, Christian B, Demeure O. Fatty acid regulation of hepatic gene transcription. J. Nutr 2005;135:2503–2506. [PubMed: 16251601]

Londos C, Sztalryd C, Tansey JT, Kimmel AR. Role of PAT proteins in lipid metabolism. Biochimie 2005;87:45–49. [PubMed: 15733736]

McGarry JD, Stark MJ, Foster DW. Hepatic malonyl-CoA levels of fed, fasted and diabetic rats as measured using a simple radioisotopic assay. J. Biol. Chem 1978;253:8291–8293. [PubMed: 711752]

McGarry JD, Mills SE, Long CS, Foster DW. Observations on the affinity for carnitine, and malonyl-CoA sensitivity, of carnitine palmitoyltransferase I in animal and human tissues. Biochem. J 1983;214:21–28. [PubMed: 6615466]

Michael MD, Kulkarni RN, Postic C, Previs SF, Shulman GI, Magnuson MA, Kahn CR. Loss of insulin signaling in hepatocytes leads to severe insulin resistance and progressive hepatic dysfunction. Mol. Cell 2000;6:87–97. [PubMed: 10949030]

Musi N. AMP-activated protein kinase and type 2 diabetes. Curr. Med. Chem 2006;13:583–589. [PubMed: 16515522]

Norris AW, Chen L, Fisher SJ, Szanto I, Ristow M, Jozsi AC, Hirshman MF, Rosen ED, Goodyear LJ, Gonzalez FJ, et al. Muscle-specific PPARgamma-deficient mice develop increased adiposity and insulin resistance but respond to thiazolidinediones. J. Clin. Invest 2003;112:608–618. [PubMed: 12925701]

Onuma H, Vander Kooi BT, Boustead JN, Oeser JK, O'Brien RM. Correlation between FOXO1a (FKHR) and FOXO3a (FKHRL1) binding and the inhibition of basal glucose-6-phosphatase catalytic subunit gene transcription by insulin. Mol. Endocrinol 2006;20:2831–2847. [PubMed: 16840535]

Pedersen TA, Bereshchenko O, Garcia-Silva S, Ermakova O, Kurz E, Mandrup S, Porse BT, Nerlov C. Distinct C/EBPalpha motifs regulate lipogenic and gluconeogenic gene expression in vivo. EMBO J 2007;26:1081–1093. [PubMed: 17290224]

Pilkis SJ, Granner DK. Molecular physiology of the regulation of hepatic gluconeogenesis and glycolysis. Annu. Rev. Physiol 1992;54:885–909. [PubMed: 1562196]

Postic C, Dentin R, Girard J. Role of the liver in the control of carbohydrate and lipid homeostasis. Diabetes Metab 2004;30:398–408. [PubMed: 15671906]

Puigserver P, Rhee J, Donovan J, Walkey CJ, Yoon JC, Oriente F, Kitamura Y, Altomonte J, Dong H, Accili D, Spiegelman BM. Insulin-regulated hepatic gluconeogenesis through FOXO1-PGC-1alpha interaction. Nature 2003;423:550–555. [PubMed: 12754525]

Qiao L, MacLean PS, You H, Schaack J, Shao J. Knocking down liver CCAAT/enhancer-binding protein alpha by adenovirus-transduced silent interfering ribonucleic acid improves hepatic gluconeogenesis and lipid homeostasis in db/db mice. Endocrinology 2006;147:3060–3069. [PubMed: 16543372]

Reisz-Porszasz S, Probst MR, Fukunaga BN, Hankinson O. Identification of functional domains of the aryl hydrocarbon receptor nuclear translocator protein (ARNT). Mol. Cell. Biol 1994;14:6075–6086. [PubMed: 8065341]

Roesler WJ, Vandenbark GR, Hanson RW. Identification of multiple protein binding domains in the promoter-regulatory region of the phosphoenolpyruvate carboxykinase (GTP) gene. J. Biol. Chem 1989;264:9657–9664. [PubMed: 2542317]

Ruderman NB, Park H, Kaushik VK, Dean D, Constant S, Prentki M, Saha AK. AMPK as a metabolic switch in rat muscle, liver and adipose tissue after exercise. Acta Physiol. Scand 2003;178:435–442. [PubMed: 12864749]

Saha AK, Vavvas D, Kurowski TG, Apazidis A, Witters LA, Shafrir E, Ruderman NB. Malonyl-CoA regulation in skeletal muscle: its link to cell citrate and the glucose-fatty acid cycle. Am. J. Physiol 1997;272:E641–E648. [PubMed: 9142886]

Saltiel AR, Kahn CR. Insulin signalling and the regulation of glucose and lipid metabolism. Nature 2001;414:799–806. [PubMed: 11742412]

Schmoll D, Wasner C, Hinds CJ, Allan BB, Walther R, Burchell A. Identification of a cAMP response element within the glucose- 6-phosphatase hydrolytic subunit gene promoter which is involved in the transcriptional regulation by cAMP and glucocorticoids in H4IIE hepatoma cells. Biochem. J 1999;338:457–463. [PubMed: 10024523]

Semenza GL. Regulation of mammalian O2 homeostasis by hypoxiainducible factor 1. Annu. Rev. Cell Dev. Biol 1999;15:551–578. [PubMed: 10611972]

Sinal CJ, Tohkin M, Miyata M, Ward JM, Lambert G, Gonzalez FJ. Targeted disruption of the nuclear receptor FXR/BAR impairs bile acid and lipid homeostasis. Cell 2000;102:731–744. [PubMed: 11030617]

Tomita S, Sinal CJ, Yim SH, Gonzalez FJ. Conditional disruption of the aryl hydrocarbon receptor nuclear translocator (Arnt) gene leads to loss of target gene induction by the aryl hydrocarbon receptor and hypoxia-inducible factor 1alpha. Mol. Endocrinol 2000;14:1674–1681. [PubMed: 11043581]

Yoon JC, Puigserver P, Chen G, Donovan J, Wu Z, Rhee J, Adelmant G, Stafford J, Kahn CR, Granner DK, et al. Control of hepatic gluconeogenesis through the transcriptional coactivator PGC-1. Nature 2001;413:131–138. [PubMed: 11557972]

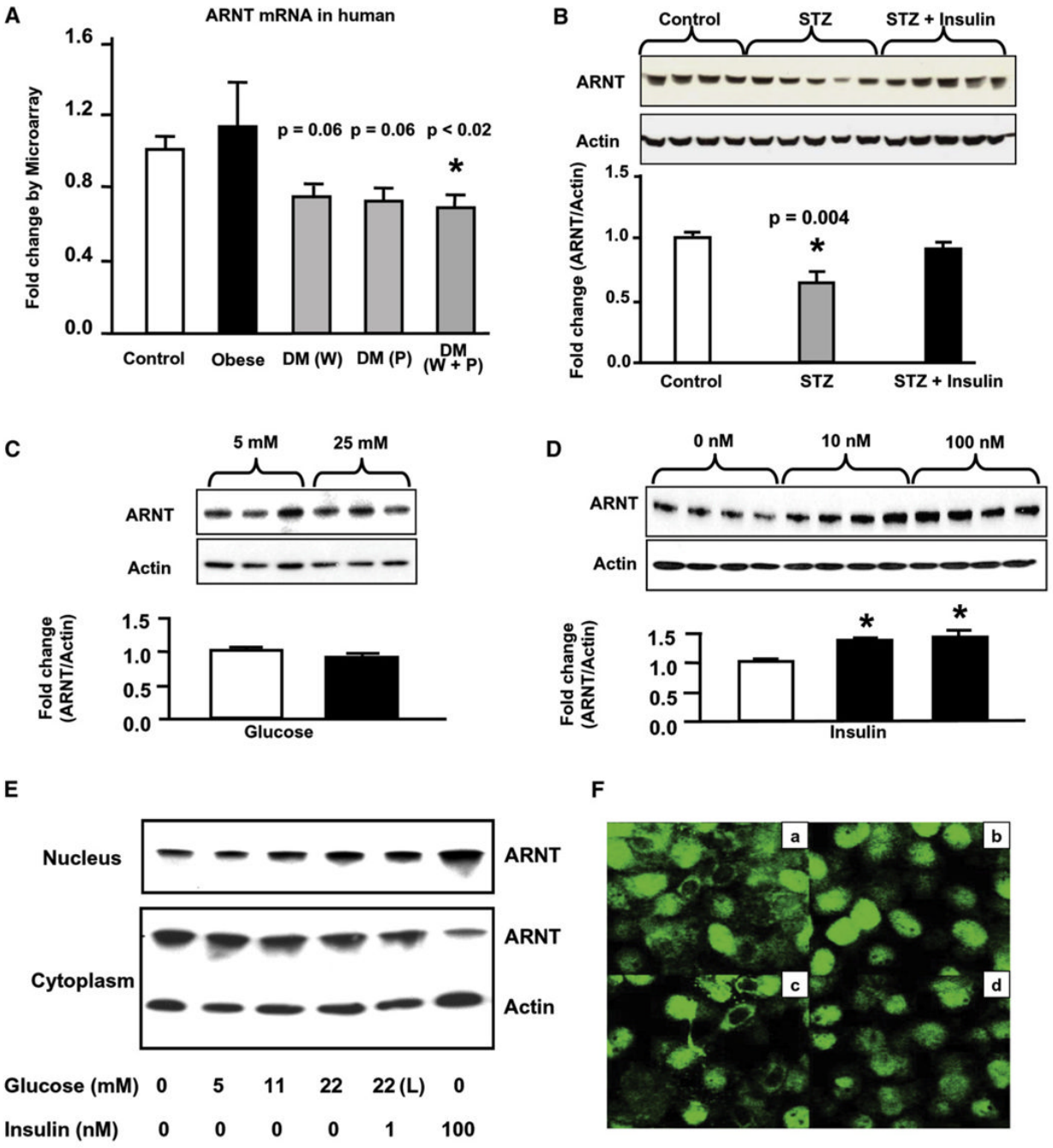

Figure 1. Regulation of ARNT Expression in the Liver of Human and Mouse Models of Diabetes

(A) Microarray analysis of ARNT expression in the individuals with lean body mass, obesity, and type 2 diabetes with well-controlled and/or poorly controlled blood glucose levels. Gene expression data were normalized with U133A Affymetrix internal gene expression parameters. The ARNT probe set is 218221_at on human genome U133A array. DM (W) and DM (P) represent type 2 diabetes with well-controlled and poorly controlled glucose, respectively. DM (W + P) presents the pooled results of DM (W) and DM (P). Data are means ± SEM of values from each group. Asterisks indicate $p < 0.02$.

(B) Expression of ARNT protein in the livers of STZ-induced male diabetic mice with or without insulin administration. Protein extracts from liver samples were analyzed by

immunoblotting for ARNT as described in the Experimental Procedures. Each lane represents the liver protein extract from an individual mouse. Data are means ± SEM of values from four or five mice. Asterisks indicate $p = 0.004$.

(C) Effect of glucose on the expression of ARNT. Human hepatoblastoma (Huh7) cells were treated with 5 mM and 25 mM glucose for 16 hr, and extracts were western blotted for ARNT as described in the Experimental Procedures. Data are means ± SEM of values from three experiments.

(D) Effect of insulin on the expression of ARNT. Huh7 cells were treated with 10 nM and 100 nM insulin for 16 hr. Data are means ± SEM of values from four experiments. Asterisks indicate $p < 0.05$.

(E) Effect of glucose and insulin on nuclear localization of ARNT. Huh7 cells were treated with glucose at 0 mM, 5 mM, 11 mM, and 22 mM; 22 mM L-glucose; or 100 nM insulin for 5 min. Protein extracts from nucleus and cytoplasm fractions of these cells were isolated and analyzed by immunoblotting for ARNT as described in the Experimental Procedures. Data are representative of 3–5 independent experiments.

(F) Effect of insulin on ARNT subcellular translocation. Huh7 cells were incubated with 10 nM and 100 nM insulin for 5 min. They were then fixed and incubated with an antibody against ARNT at 4°C for 24 hr and were subsequently blotted with GFP-conjugated IgG (Jackson Laboratory) for 1 hr at room temperature in the dark. The cells were evaluated using fluorescent microscopes. Subpanels (a) and (b) represent cells treated with 0 nM and 10 nM insulin, respectively. Subpanels (c) and (d) represent cells treated with 0 nM and 100 nM insulin. Data are representative of three independent experiments.

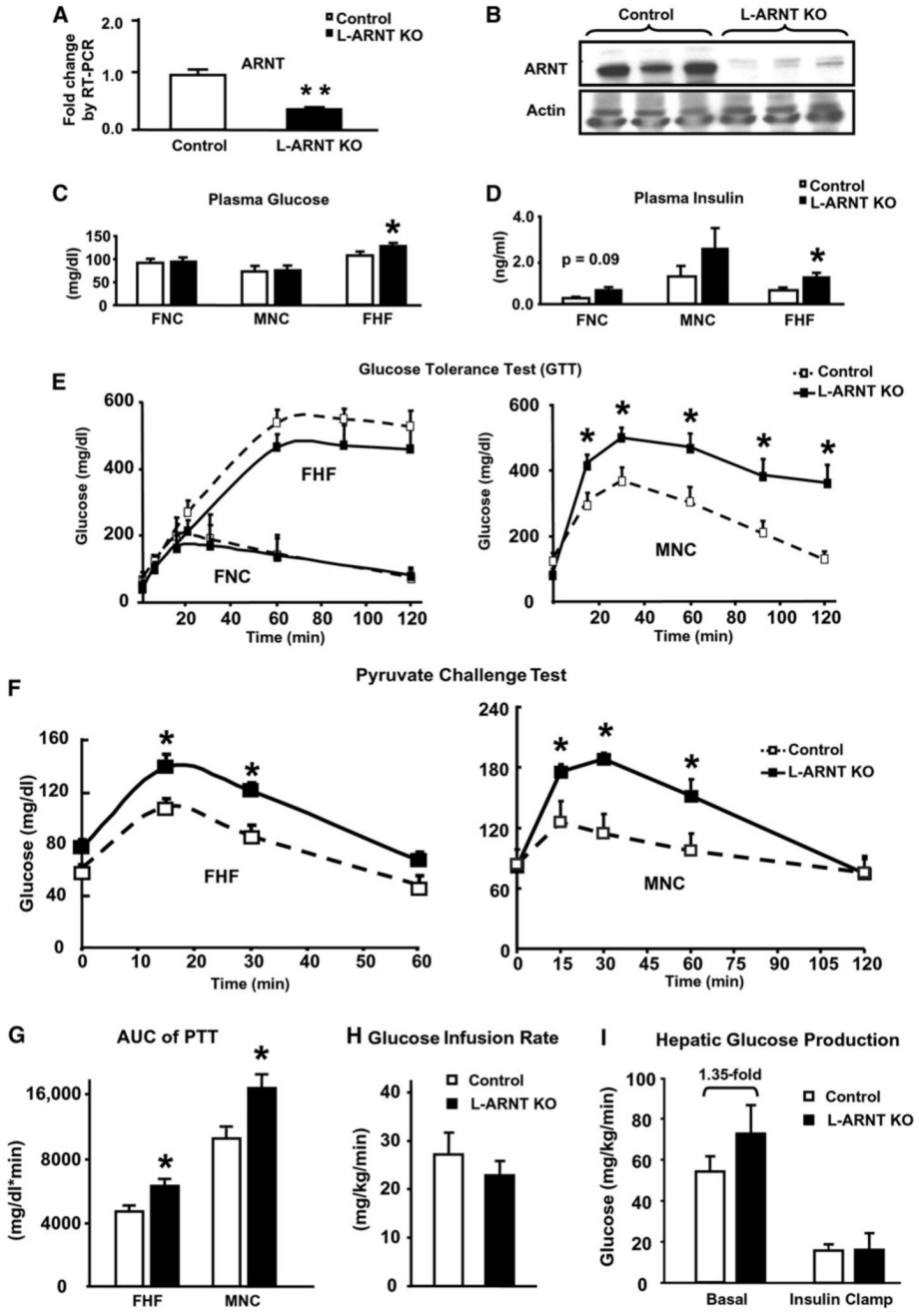

Figure 2. Glucose Metabolism in the Mice with Acute Liver-Specific Ablation of ARNT

(A) The ARNT flox/flox mice were injected via the tail vein with adenovirus Ad-Cre vector to knock out ARNT in liver (L-ARNT KO). Age- and sex-matched ARNT flox/flox mice were injected with Ad-CMV as controls (Control). Six days after injection, hepatic mRNA levels of ARNT were measured by real-time RT-PCR.

(B) ARNT protein levels were measured from a 30 mg aliquot of total homogenates from liver by western blot analysis. Each lane represents the liver sample from an individual mouse.

(C and D) Fed blood glucose and insulin levels were measured in Control and L-ARNT KO mice from the FNC, FHF, and MNC groups.

(E) Glucose tolerance tests (GTTs) were performed in Control and L-ARNT KO mice from the FNC, FHF, and MNC groups.
(F) Pyruvate challenge tests in Control and L-ARNT KO mice from the FHF and MNC groups were used to assess hepatic gluconeogenesis.
(G) The area under the curve (AUC) for serum glucose during the pyruvate challenge tests from FHF and MNC groups were calculated using the linear trapezoidal rule, subtracting the baseline value from each time point.
(H) Glucose infusion rates for Control and L-ARNT KO mice from the FNC group during the euglycemic clamp were measured.
(I) Basal and insulin-suppressed hepatic glucose production in Control and L-ARNT KO mice from the FNC group were measured during the euglycemic clamp. The black line with black boxes in the figure represents the data obtained from L-ARNT KO mice. The dotted line with open boxes in the figure represents the data obtained from Control mice. Data are means ± SEM of values from five or six mice. Asterisks indicate $p < 0.05$. Data from Figures 2C–2I are means ± SEM of values from five or six mice. Asterisks indicate $p < 0.05$.

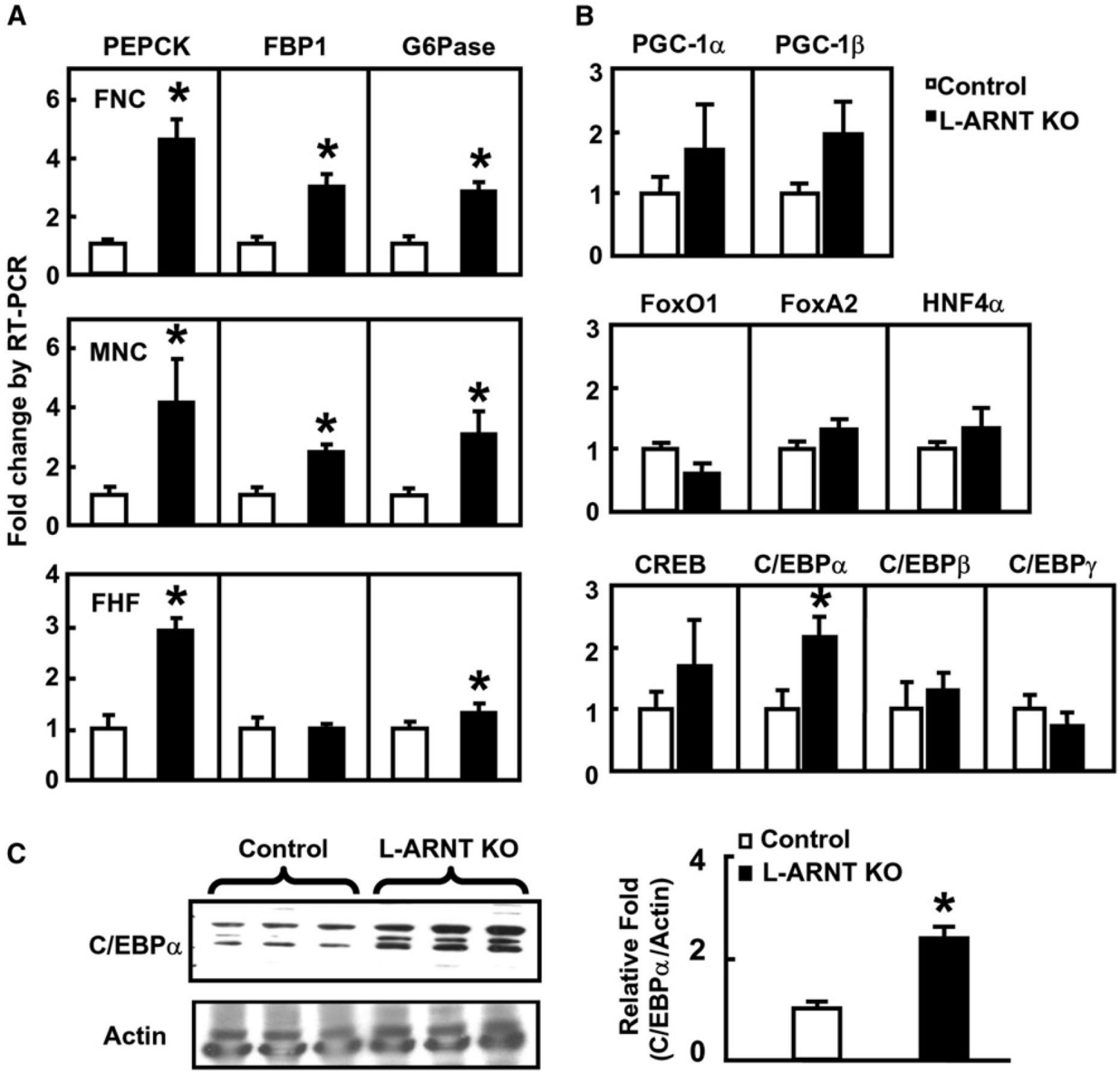

Figure 3. Effect of L-ARNT KO on the Expression of Hepatic Gluconeogenic Enzymes

(A) mRNA levels of gluconeogenic genes from the livers of the three experimental groups were measured by real-time RT-PCR. The livers of mice from each group were obtained in the fed stage at day 6 after injection. Data are representative of results obtained from five or six mice in each group.

(B) mRNA levels of transcription factors and coactivators involved in the regulation of PEPCK, G6Pase, and FBP1 were measured by real-time PCR. Data are representative of results obtained from six mice in the FNC group.

(C) C/EBPα protein level was measured by immunoblotting in the livers of L-ARNT KO mice from the FNC group. Each lane represents the liver protein extract from an individual mouse. Quantification data of C/EBPα protein were obtained from five mice. Asterisks indicate $p < 0.05$.

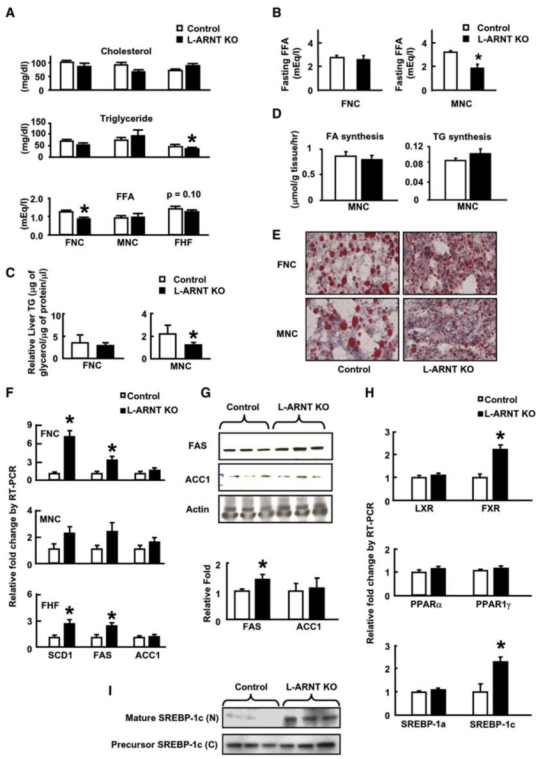

Figure 4. Effect of L-ARNT KO on Hepatic Lipid Metabolism

(A) Serum cholesterol, triglyceride (TG), and FFA levels in Control and L-ARNT KO mice from the FNC, FHF, and MNC groups in the fed condition.

(B) Fasting serum FFA level in Control and L-ARNT KO mice from the MNC group.

(C) Liver TG levels in Control and L-ARNT KO mice from the FNC and MNC groups.

(D) Fatty acid and TG synthesis in the livers of Control and L-ARNT KO mice from the MNC group. Data from Figures 4A–4D are representative of results obtained from five or six mice in each group. Asterisks indicate $p < 0.05$.

(E) Oil red O staining of liver slides of Control and L-ARNT KO mice from the FNC and MNC groups. Data are representative of five or six independent experiments.

(F) mRNA levels of lipogenic genes in the livers of Control and L-ARNT KO mice from the FNC, MNC, and FHF groups under the fasting condition.

(G) Protein levels of ACC1 and FAS were measured by western blot in the livers of Control and L-ARNT KO mice from the FNC group.

(H) mRNA levels of transcription factors and coactivators involved in the regulation of lipogenic genes in the livers of Control and L-ARNT KO mice from the FNC group. Data from Figures 4F–4H are representative of results obtained from five or six mice in each group. Asterisks indicate $p < 0.05$.

(I) Total and mature SREBP-1c protein levels were measured by immunoblotting in the livers of L-ARNT KO mice from the MNC group. Each lane represents the liver protein extract from an individual mouse. Data are representative of results obtained from 3–6 mice in each group. Asterisks indicate $p < 0.05$.

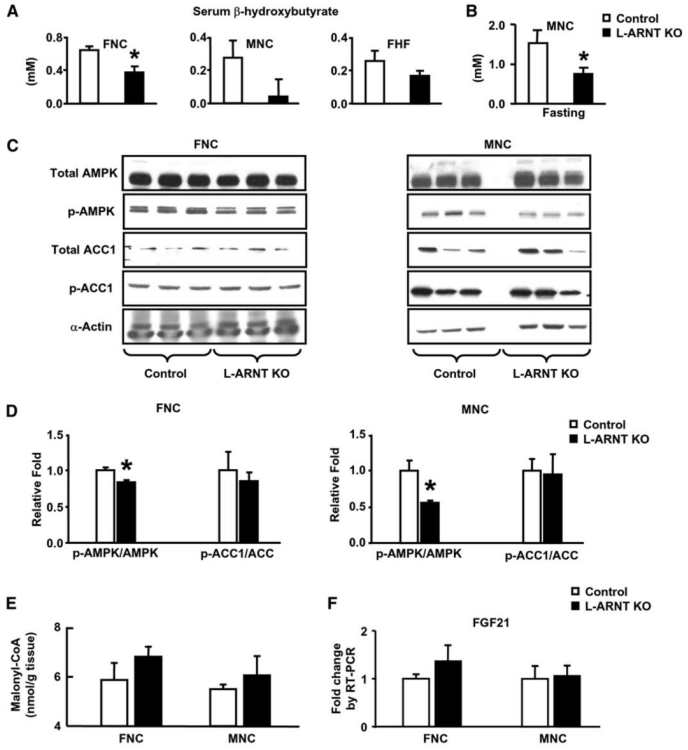

Figure 5. Effects of L-ARNT KO on Hepatic Fatty Acid β-Oxidation and Ketogenesis

(A) Fed serum β-hydroxybutyrate (β-OHB) levels in Control and L-ARNT KO mice from the FNC, MNC, and FHF groups.

(B) Fasting serum β-OHB levels in Control and L-ARNT KO mice from the MNC group.

(C) Total and phosphorylation levels of AMPK and ACC1 proteins were measured by western blotting in the livers of Control and L-ARNT KO mice from the FNC and MNC groups.

(D) Quantification of protein ratio of p-AMPK/AMPK and p-ACC/ACC in the livers of Control and L-ARNT KO mice from the FNC and MNC groups.

(E) Malonyl-CoA levels in Control and L-ARNT KO mice from the FNC and MNC groups.

(F) mRNA levels of FGF21 genes in the livers of Control and L-ARNT KO mice from the MNC group. Data are representative of results obtained from five or six mice in each group. Asterisks indicate $p < 0.05$.

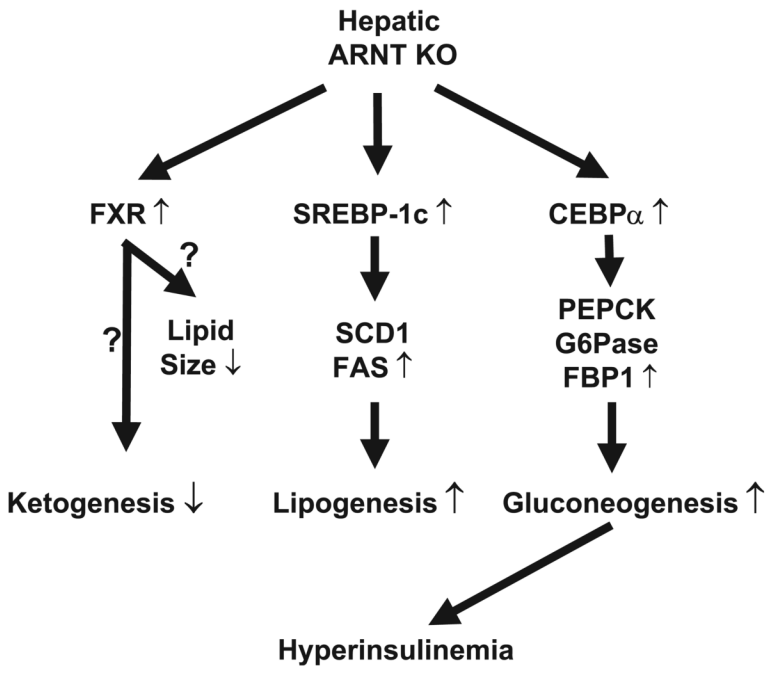

Figure 6. A Possible Model of ARNT Reduction in Liver

ARNT reduction in liver increases fed insulin levels and elevates hepatic gluconeogenesis. In parallel, expression of key gluconeogenic enzymes, such as PEPCK, G6Pase, and FBP1, is increased. ARNT reduction in liver also changes hepatic lipid size and activation of lipogenesis process, possibly due to elevated expression of genes encoding FXR, SREBP-1c, FAS, and SCD1.

Table 1

Clinical and Biochemical Data Obtained from Individuals with Lean Body Mass, Obesity, and Type 2 Diabetes with Both Well-Controlled and Poorly Controlled Blood Glucose Levels

Human liver samples were obtained from volunteers undergoing elective cholecystectomy (lean subjects) and gastric bypass surgery (morbidly obese with or without type 2 diabetes).

	Lean Control	Obese	Obese DM Well Controlled (DM [W])	Obese DM Poorly Controlled (DM [P])
Subjects per group	5	4	7	4
Age (years)	36 ± 12	39 ± 11	45 ± 12	43 ± 14
Gender	5 F	1 M / 3 F	2 M / 5 F	2 M / 2 F
BMI (kg/m^2)	24 ± 5	52 ± 4^a	53 ± 9^a	55 ± 4^a
Fasting glucose (mg/dl)	86 ± 14	88 ± 9	135 ± 35^a	211 ± 87
Fasting insulin (μU/ml)	6.3 ± 5.6	21.7 ± 20.8	25.0 ± 20.3	72.9 ± 48.6
HOMA-IR	1.5 ± 1.4	5.0 ± 5.4	8.5 ± 7.4	38.5 ± 31.9
SI (insulin sensitivity)		0.9 ± 1.5	0.8 ± 0.9	0.1 ± 0.2
Hemoglobin A1C (%)	5.4 ± 0.3	5.2 ± 0.1	6.3 ± 0.6^a	9.9 ± 1.1^a
Liver lipid (% of area)	2.4 ± 3.1	9.8 ± 17.6	15.2 ± 13.2	9.3 ± 4.9

^{a}Indicates $p < 0.05$ compared with lean control.